TRANSPORT AND TRAPPING OF WOODY DEBRIS IN A RIVER MEANDER PROTECTED WITH ELJ GROYNES

W. CHUAN[1], J.M. KUROIWA[2], L.F. CASTRO[3], & L. VASQUEZ[4]

[1] Former Student. Universidad Nacional de Cajamarca. Cajamarca, Peru.
[2] Director. National Laboratory of Hydraulics & Professor, School of Civil Engineering. Universidad Nacional de Ingenieria. Lima, Peru.
[3] Researcher. National Hydraulics Laboratory. Universidad Nacional de Ingenieria. Lima, Peru.
[4] Director. School of Hydraulic Engineering. Universidad Nacional de Cajamarca. Cajamarca, Peru.
wchuanh@unc.edu.pe, jkuroiwa@uni.edu.pe, lfcastro@uni.edu.pe, lvasquez@unc.edu.pe

ABSTRACT

Exploratory tests were conducted to observe the effects of incoming Large Wood Debris (LWD) on Engineered Log Jams (ELJ) groynes' stability and permeability and the capacity of an ELJ groyne field, built on the outer bank of a river meander, to trap LWD and establish new habitat. An existing experimental facility, where a 4.2 km curved section of an Amazonian river was modeled at a 1/60 scale, was used to simulate transport and retention patterns of LWD. Bed material was sand, slope was 0.22 per one thousandth and flow was subcritical in all tests. Radius of curvature to width ratio was approximately 2. Wood dowels of different sizes were incorporated into the flow using a manual conveyor belt and trajectories were recorded with video cameras mounted on a drone and on both sides of the testing flume. When ELJ groynes were fully submerged at peak flows, no simulated logs were captured by the ELJ groyne field. When ELJ groynes remained unsubmerged throughout the tests, with flows representing 25 and 50-year-floods, between 8 and 14 % of the of the simulated logs were trapped mostly near the upstream face of the ELJ groynes. Therefore, an ELJ groyne field placed on the outer bank of a curved section holds potential for supply new material over time for rehabilitating erosion control structures and forming new riverine habitats. In addition, LWD did not appear to affect ELJ groynes stability or permeability, at least in laboratory tests.

Keywords: Large Wood Debris (LWD), river hydrodynamics, Engineered Log Jams (ELJ), riverine habitat restoration, groynes.

1 INTRODUCTION

Bank erosion and river migration threaten infrastructure located near riverine areas. INDECI (2006) identified a sector of the Madre de Dios River in which the outer bank of a river bend was migrating laterally at a 2-4 m/yr rate. The Interoceanic Highway was threatened by river migration and a number of solutions were proposed and tested in a physical model. Shields (2004) tested the use of Large Wood Debris Structures (LWDS) in a stream that drained a 37-km^2 basin and recommended the use of LWDS in small streams in the Unites States of America.

Floating wooden debris is often dragged by rivers during high flows. Flooding associated with intense rain events in relatively dry zones can wash out fallen trees or deadwood (Pfister et al. 2013). Also, bank erosion is an important process of wood supply (Murphy & Koski 1989, cited by Gurnell et al. 2002) because destructive forces of the streams erode away toes of forested banks so that entire trees are destabilized and fall into the stream (Pfister 2013, Wohl 2013, Abbe et al. 2003). Woody debris can damage important infrastructure built along the stream or located at river crossings. Extraction of this type of material could be a difficult task because it accumulates after a major flood occurs (Ruiz-Villanueva 2014). In the Amazon jungle transport of woody debris is very high during the rainy season. Flow surface is totally covered by tree logs for several days during floods making river navigation hazardous (Consorcio Hidrovia Huallaga 2005). Interest in the dynamics of woody debris started by the end of the 20th century (McDonald et al 1982). Braudrick and Grant (2000) modeled the simplest case: a cylindrical log in a uniform field floating above a flat bed. Experiments showed that the most important factors related to log motion entrainment are piece angle relative to flow direction, whether or not the log had a rootwad, the density of the log, and the piece diameter.

Use of LWD for implementing bank erosion control measures could be a logical solution in the lowlands of the Amazon Basin where forest resources and woody necromass are abundant. However, basins are usually large, in the order of thousands of square kilometers and collecting raw material may be costly.

A series of experiments were carried out to find a configuration that reduces scour both on the outer bank of a river bend and the training structures. ELJ groynes were placed on the outer bank of a physical model and configuration changed slightly between tests. Further details can be found in Jacay (2019). Exploratory tests to assess the groyne field capacity to capture floating logs were included as part of the experimental program and analyzed in Chuan (2019). This article summarizes results of the experimental phase of a

research program in which a physical model of an Amazonian river was used to study deposition patterns of large woody debris in the river bend of a meandering sector.

2 METHODOLOGY

Tests described in this article were part of a broader experimental program whose main objective was to assess the effectiveness of ELJ groynes to control erosion in the outer bank of a river bend. Prediction of geomorphic changes in the river bed due to the construction of ELJ groynes was also a component of the research program. A hydraulic model, that represented a 4.2 km stretch of the Madre de Dios River, was built to test several erosion control methods in the right bank of the river in a sector called La Pastora-Puerto Maldonado, in SE Peru, near the Peru-Brazil-Bolivia border. Banks were being eroded away and the river thalweg was approaching the Interoceanic Highway and compromising infrastructure of Puerto Maldonado, capital of the Madre de Dios Region. Figure 1, below, shows a plan view of the area.

Figure 1. View of the Madre de Dios river meander located in risk zone "La Pastora-Puerto Maldonado". Source: Google Earth / Insert: OEC (2017)

The number of simulated LWD elements was determined based on the potential areas affected by heavy rains and large floods that erode away river banks and adjacent forested areas. Available tree necromass in the vicinity of the river was also accounted for as an input. GIS was used to map and identify areas prone to excessive scour that may lead to tree detachment from soil.

Hydrological and previous botanical studies by Aragâo (2009) and Araujo-Murakami (2011) were taken into account when estimating the number of elements that were going to be incorporated into the flow. Further details are included in Chuan (2019). Trunk diameters and lengths were in the order of 0.24 to 0.54 m and 3.12 to 7.02 m, respectively. Approximately 19 % of the LWD elements had roots, so disks of varying sizes were attached to them. Scaled down roots and log dimensions were determined based on the works of Braudrick et al. (1997), Gurnell et al. (2002), Shields (2004) and Chao et al. (2009). As it may be very impractical to model a large number of elements, it was decided to simulate a short period of time of LWD transport and document the experiments with still photography and video cameras for posterior analysis. This component is basically exploratory and experimental as it was intended to visualize transport and retention patterns of LWD in a river bend. In particular, trapping of simulated LWD was of interest as trapped wood could be used to replace or reinforce material in existing ELJ structures and allow formation of riverine habitat. An existing 1/60 scale live-bed hydraulic model that represented a curve sector of the Madre de Dios River was used to implement tests that also included simplified tests of LWD transport. In all simulations logs floated. As a result, no gravitational or frictional forces were present as it was conceptualized by Braudick and Grant (2000). Therefore, trunk and root dimensions were reduced to the model scale taking into account simplifications made by Braudrick et al. (1997) and Gurnell et al. (2002). Groyne configurations corresponded to two settings oriented to optimize protection of the outer bank under design conditions. Descriptions and outcomes of the tests follow.

3 EXPERIMENTAL FACILITIES, EQUIPMENT, MATERIALS AND PROCEDURES

3.1 Experimental setup and procedures

Tests were conducted in an undistorted physical model of approximately 70 m long that represented a 4.2 km reach of the Madre de Dios River in SE Peru. This model was initially used for studying erosion control measures to protect the right bank of the river. Water was stored in an underground reservoir located below the Didactic Division building whose capacity was 80 m^3. Five sump pumps with a nominal maximum conveying capacity of 760 L/s were used to convey flows to an elevated rectangular reservoir, built 5 m above

ground. The maximum capacity of the elevated reservoir was 27 m^3. An overflow pipe returned excess discharge to the underground reservoir. Flow was controlled by a 356 mm steel slide gate and a 50 mm by-pass valve was used to adjust target discharges. Engineered Log Jam groynes (labeled E-1 through E-12) in the downstream direction in Figure 2 were placed on the right bank of the testing flume. The flume was covered with sand whose d_{50} and standard deviation were 0.4 mm and 1.6, respectively. The right bank, which is very steep in study site, was made of a thin layer of concrete placed over a thin layer of clay and compacted wet sand so that any small settlement may reflect on bank cracking.

The sand bed was setup with reference points and elevations. The hydraulic model was confined by perimetric brick walls that were reinforced with brick buttresses. Cross sections data were extracted from ADCP bathymetric surveys in submerged reaches and total station surveys for land surveys. Survey markers were used to make both sources of information compatible. Average bed slope was 0.22 per 1 thousandth.

One upstream movable steel platform was used to inject tracers, styrofoam balls and floating debris. This platform was usually located just downstream of the stilling basin. Another movable steel platform was used to mount a limnimeter, to measure ground and water levels, and an Acoustic Doppler Velocimeter (ADV) to record 3D velocity fields. Water depths and velocity fields were taken at 11 selected cross sections. Figure 2 shows an aerial view of the experimental facility for Test 3, described in the next sections. Groynes are labeled as E-i. The underscore "i" indicates the relative position of the groynes.

Capirona (Calycophyllum spruceanum) whose average density is 760 Kg/m^3, was used to model floating logs. In this project maximum height of this species ranges between 15 and 35 m and trunk diameters were considered to be between 0.5 and 1.5 m. Density obtained by direct measurement of mass and volume was close to 710 Kg/m^3.

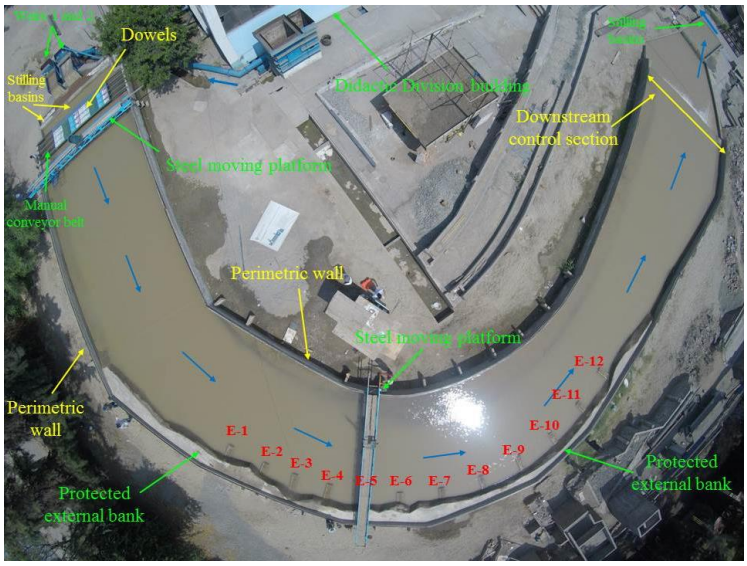

Figure 2. View of experimental module. This 1/60 hydraulic model represents 4.2 km of the Madre de Dios River in SE Peru. The setup is shown for experiments 1 and 3.

Simplifications made by Braudrick and Grant (2000) were taken into account when designing scale down logs. Submerged depth was estimated considering full flotation. Dowels, that simulated fallen trees, were assigned different dimensions to represent variability in length and sizes that may be observed in a flood. LWD may or not have roots. Rootless logs were cylindrical wood dowels made up of Capirona. Table 1, shown below, includes dimensions of dowels that simulate rootless logs at a 1/60 scale. L_t is the total length of the simulated wood, D_t and A_t are dowel diameter and cross sectional area. Variables h and A_{sub} represent submerged depth and area, respectively.

Table 1. Dimensions of rootless logs that are to be incorporated into the flow.

Nº	Color, size	L_t (cm)	D_t (cm)	A_t (cm^2)	h (cm)	A_{sub} (cm^2)
1	White, large	11.70	0.90	0.64	0.60	0.45
2	Pink	10.40	0.80	0.50	0.53	0.36
3	Light blue	7.80	0.60	0.28	0.40	0.20
4	Green	6.50	0.50	0.20	0.33	0.14
5	White, short	5.20	0.40	0.13	0.27	0.09

Floating logs were modeled as thin, long, cylinders attached to a disk, whose dimensions can be seen in Table 2, below, where: L_t is the length of the long cylinder, D_t is its diameter, D_{rw} is the diameter of the disk (simulated rootwad) and h_1 y h_3 are the submerged depths of the cylinder and disk, respectively.

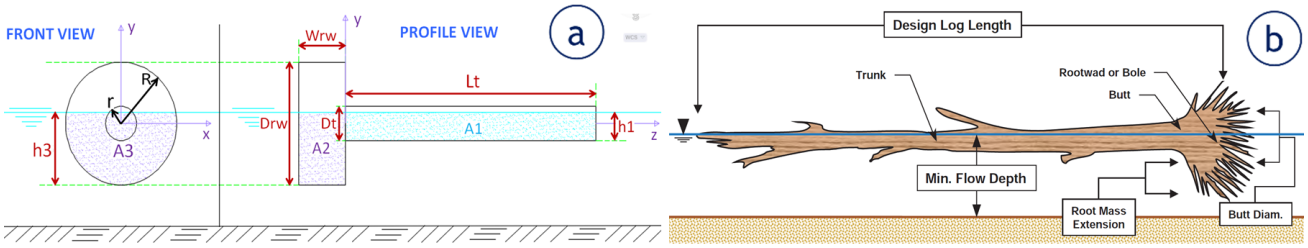

Figure 3. a) Characteristic dimensions of an element in full flotation. b) Schematic of log length and root mass extension when only flotation is considered (NCHRP 2010).

Table 2. Dimensions of simulated fallen trees with roots.

		Dowel dimensions					Disk Dimensions						
Nº	**Color, size**	**L_t (cm)**	**D_t (cm)**	**h_1 (cm)**	**A_1 (cm^2)**	**Vol_1 (cm^3)**	**Wrw (cm)**	**Drw (cm)**	**h_3 (cm)**	**A_2 (cm^2)**	**A_3 (cm^2)**	**Vol_{rw} (cm^3)**	**Vol_2 (cm^3)**
1	White, large	11.70	0.90	0.74	8.71	5.62	1.35	2.40	1.49	2.02	2.96	6.10	3.99
2	Pink	10.40	0.80	0.65	6.81	3.90	1.20	2.00	1.25	1.50	2.08	3.77	2.49
3	Light blue	7.80	0.60	0.49	3.83	1.64	0.90	1.50	0.94	0.85	1.17	1.59	1.05
4	Green	6.50	0.50	0.42	2.71	0.97	0.75	1.40	0.87	0.65	1.00	1.15	0.75
5	White, short	5.20	0.40	0.34	1.76	0.51	0.60	1.20	0.74	0.44	0.73	0.68	0.44

Table 3, below, shows the final number of logs (without roots) or trees (with roots) incorporated into the flow.

Table 3. Number of elements incorporated into the flow. Most of the elements were rootless (without disk), whereas 19 % had disks at the base.

Nº	**Color, size**	**Quantity**		**Subtotal**
		Without disk	**With disk**	
1	White, large	155	52	207
2	Pink	413	103	516
3	Light blue	1550	413	1963
4	Green	3100	827	3927
5	White, short	5166	1085	6251
			Total:	**12864**

Logs were incorporated into the flow using a manual conveyor belt. Dowels were spread in a rectangular area whose length in the direction of the flow and width were 6 m and 10 m, respectively. Rate and timing of incorporation of logs into the flow was carefully taken into account to represent a net inflow of logs into the river during high flows. Several video cameras registered each experiment including one mounted on a drone. A High Definition video camera was used to register flow trajectories from the right bank during each experiment. Flow trajectories were recorded using a Hero Go Pro camera mounted on a quadcopter drone. Both videos and still photographs were taken. Flight time of the drone was limited to approximately 20 to 25 minutes. Still photographs and videos were also taken on the ground before, during and after the tests. Fluorescein, dissolved in water, was injected using a perforated half pipe to uniformly spread the tracer into the flow. Floating logs were released using the conveyor belt located near the upstream end of the hydraulic model. Discharges tested were 466 and 514 L/s. By the end of the test, the main valve was slowly shut down and the testing module drained. Laser 3D scanning was conducted for detecting changes in the bed topography and analyze scour and deposition patterns. Scanning of the bed took place one or two days after each experiment was concluded.

4 DATA COLLECTION AND MAIN OBSERVATIONS

4.1 Description of tests and outcomes

Tests described in this document are part of a larger experimental program. Only the tests in which LWD were incorporated into the flow are included in this section and were conducted between October 2016 and February 2017. In the first test ELJ groynes were fully submerged whereas in the second and third tests flow was unsubmerged. The number of simulated logs was constant for all tests. A total of 12 864 dowels were incorporated into the flow at a rate of 201 pieces/s using the manual conveyor belt located upstream of the testing area. No logs were trapped in the submerged test. Trapping of logs occurred in the second and the third test. Figure 3d, 3e and 3f, below, show a sequence of a mass of injected tracer passing through the river

bend. It can be clearly seen that the tracer separates from the left bank and the entire mass approaches the right bank (Figure 4). This observation will be compared with the simulated LWD flow patterns in the experiments described in this article.

It was observed that, in most cases, simulated LWD elements longest axis was approximately parallel to the main flow direction. These elements change direction when passing by the tip of an ELJ groyne, where they were diverted towards the main stream. Entrainment took place after accumulated LWD was impacted by an incoming element. Impact caused the detachment of one or more units from the jammed wood debris. In tests 2 and 3 simulated LWD elements got jammed mostly in the upstream face of a groyne or in the adjacent area along the outer bank. The rest of the LWD was deposited near where the structure was anchored to the bank (embedment areas).

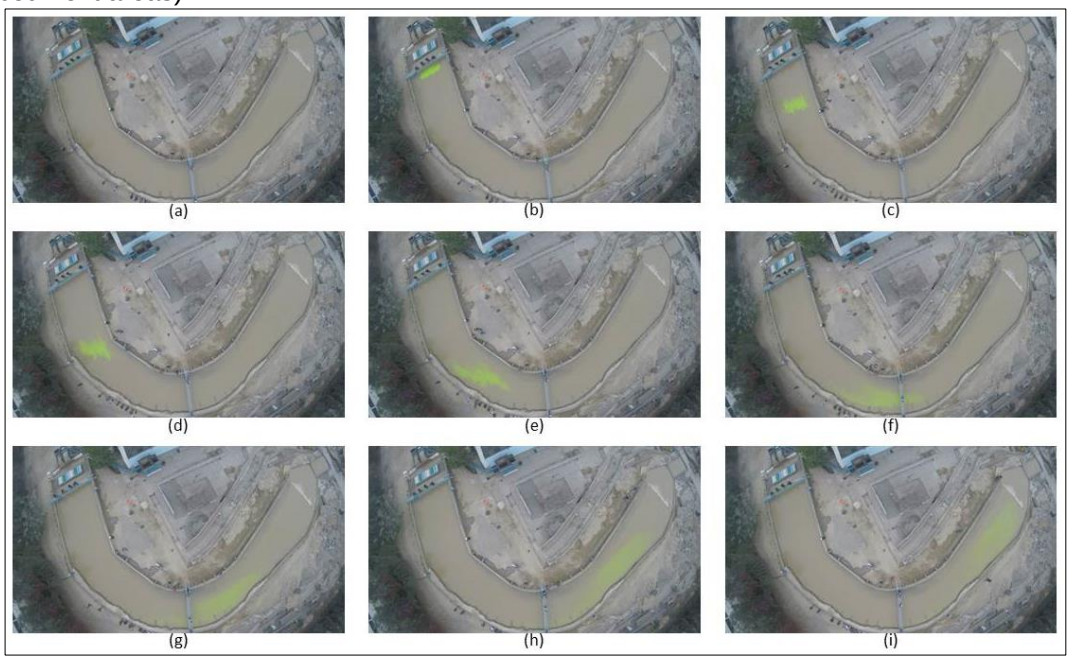

Figure 4. Sequence of tracer passing through the river bend.

First test – Submerged groynes

The first test was conducted con October 27, 2016. Twelve ELJ groynes were placed on the right bank at a 90º. Target discharge was 466 L/s and groynes were submerged when the target discharge was applied. No logs were trapped upstream of the groynes, between groynes or in the modeled river floodplains in this test as structures were submerged and logs floated above the erosion control structures. A few dowels were temporarily retained by vertical elements that emerged above the water level. However, local vorticity rapidly released the logs from the structures and any element that may have been deposited in the outer bank.

Figure 5a, below, shows the initial alignment of dowels, upstream of the curved section. In lighter color are shown alignments A, B and C. A is closer to the right bank. Alignment M and N are located between A and B and B and C, respectively. As the flow moves downstream, C, where water depth is lower, moved faster even in the straight reach upstream of the river bend, and approached the right bank. Therefore, shortly after simulated LWD was released by the manual conveyor belt most units were displaced to the right bank by the flow. However, no trapping was recorded as groynes were fully submerged. Therefore, no further information is included in this article. It can be concluded that a groyne field should not be submerged for the design condition if the objective is trapping of floating LWD.

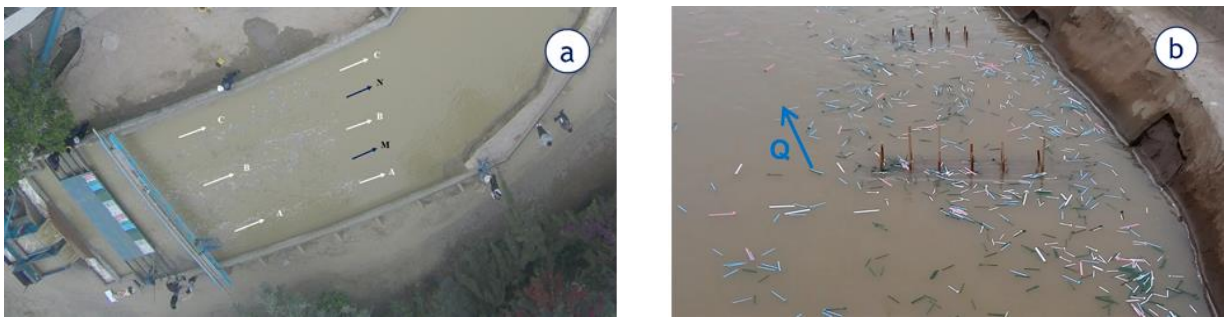

Figure 5. a) Initial position of alignments A, B, C, M and N. b) Passage of dowels through the ELJ groyne field. Centrifugal force pushes LWD elements toward the right bank.

Second test – Unsubmerged test

This test was conducted on December 20, 2016 and 11 ELJ groynes were placed on the right bank. The first and the last structure were placed at a 120º angle with respect to the flow. The rest of the ELJ groynes were placed at 90º. Average velocity of flow in the curve was 0.36 m/s, estimated centrifugal force was 0.29 KN and estimated Froude number was 0.290. In the second test trapping patterns were evident. Alignments A, B, C, M and N upstream of the curved section remain as defined in the previous section.

Figure 6a shows lateral displacement of positions A, B, C, M and N towards the right bank, leading to convergence of the dowels along a line formed by the tips of the groynes. In Figures 6b and 6c it can be seen that simulated LWD formed an alignment that ran parallel to the bottom of the right bank near the groynes´ tips. Detail in Figure 6c shows trapping of dowels in the upstream face of groyne E-1. However, flow was diverted towards the interior of the flume and an intermittent, small vortex, was formed around the tip of the groyne. On the other hand, the strength of clockwise large vortices, formed between groynes, pulled most trapped dowels towards the main flow and they continued flowing in the downstream direction. As the flow was diverted towards the left, simulated LWD were also diverted and very few LWD units remained trapped between groynes. Intermittent, smaller vortices that pull simulated LWD into the area between groynes were also observed. E-1 sustains direct impact of the flow and simulated LWD. A chaotic pattern could be observed upstream of E-1. Detail on the left of Figure 6d shows flow pattern between E-9 and E-10. A larger, clockwise vortex can be visualized by the dowels. Notice that a triangular deposition forms between the upstream face of E-10 and the right bank where a “dead zone” is generated due to the larger, clockwise vortex between groynes E-9 and E-10. Trapped simulated LWD elements were recovered and accounted for.

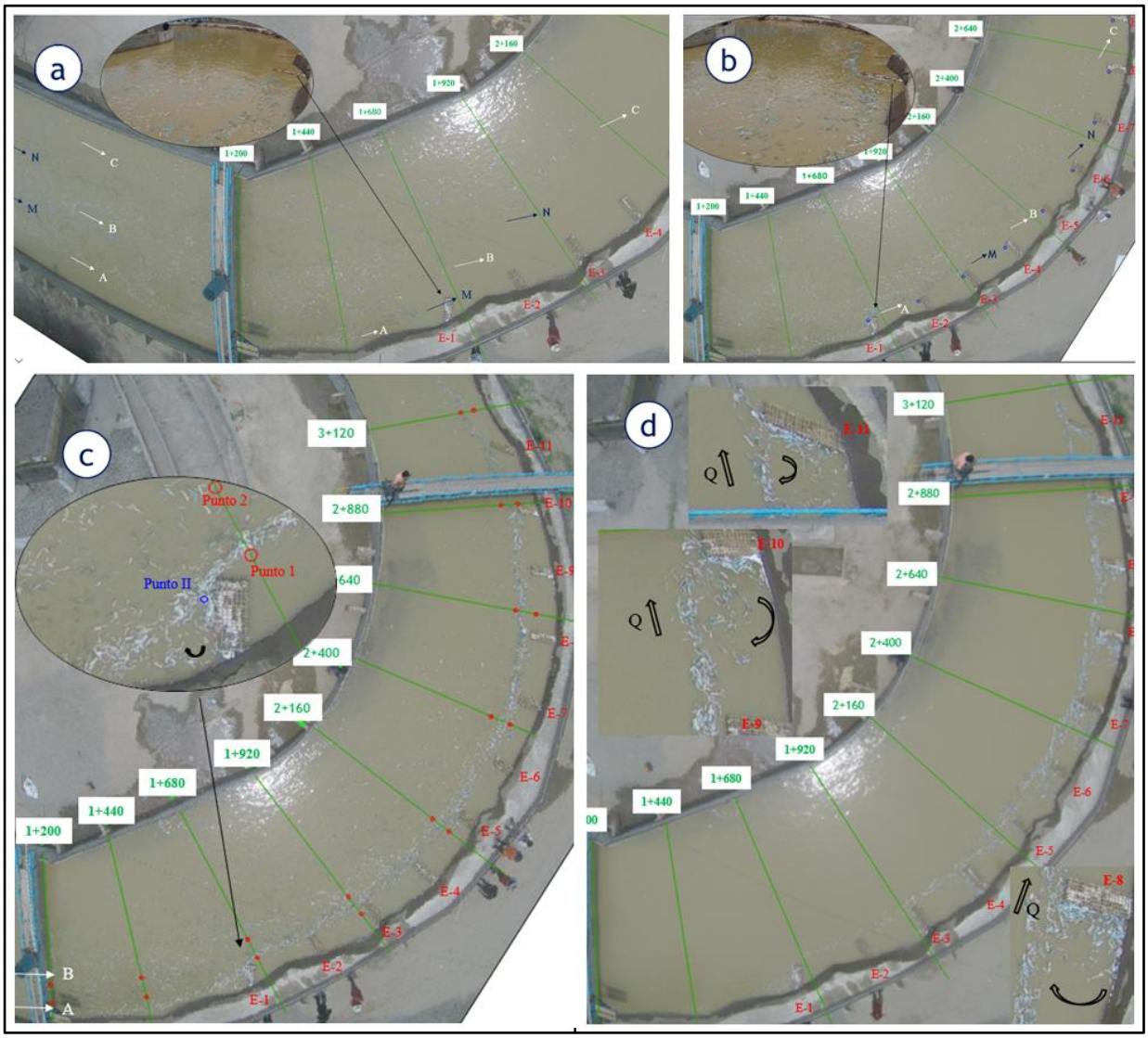

Figure 6. Displacement of simulated LWD in Test 2. Notice that most dowels move towards the right bank forming a “caravan” type of flow pattern in a very narrow strip.

Table 4 shows the number of elements trapped immediately upstream of an ELJ groyne. The largest accumulation occurred in the upstream face of E-8. One hundred and fifty-one units were trapped between E-

7 and E-8. Interestingly, the second largest accumulation of simulated LWD occurred immediately upstream of E-1. This is the first ELJ groyne and the one that sustained significant impact from passing LWD as seen in Figures 6c and 7. After the test finished, 1 024 elements were trapped in the ELJ groyne field. This is approximately 7.95 % of the total LWD that was released by the manual conveyor belt. Figure 7 (left figure), below, shows ELJ groynes E-2 trough E-5 and the right bank looking in the downstream direction. The arrow shows the flow direction. Deposition upstream of E-1, E-6, E-7, E-8, E-9 and E-10 is shown. Notice triangular accumulations of LWD immediately upstream of E-8, E-9 and E-10 in Figure 7. Sides of the triangles are the right bank and the upstream face of ELJ groynes E-8, E-9 and E-10.

Table 4. Number of simulated LWD units trapped upstream of groynes in Test 2.

ELJ Groyne		**E-1**	**E-2**	**E-3**	**E-4**	**E-5**	**E-6**	**E-7**	**E-8**	**E-9**	**E-10**	**E-11**	
Simulated LWD with disks	White, small	40	12	19	18	4	11	15	18	11	20	13	
	Green	11	--	4	14	2	9	7	20	11	17	1	
	Light blue	1	--	2	4	2	1	2	13	8	8	8	
	Pink	--	--	1	--	--	--	--	--	1	--	--	
	White, large	--	--	1	1	--	--	--	--	--	--	--	
Simulated LWD without disks	White, small	71	52	51	60	7	8	20	56	14	55	8	
	Green	24	5	27	38	14	14	17	30	6	29	7	
	Light blue	2	--	5	5	4	3	12	13	8	7	7	
	Pink	--	--	2	--	--	2	2	--	1	2	--	
	White, large	--	--	--	--	--	--	1	1	--	1	3	**Total trapped**
Partial quantity		149	69	112	140	33	48	76	151	60	139	47	1024
Partial % of total		1.16	0.54	0.87	1.09	0.26	0.37	0.59	1.17	0.47	1.08	0.37	7.96

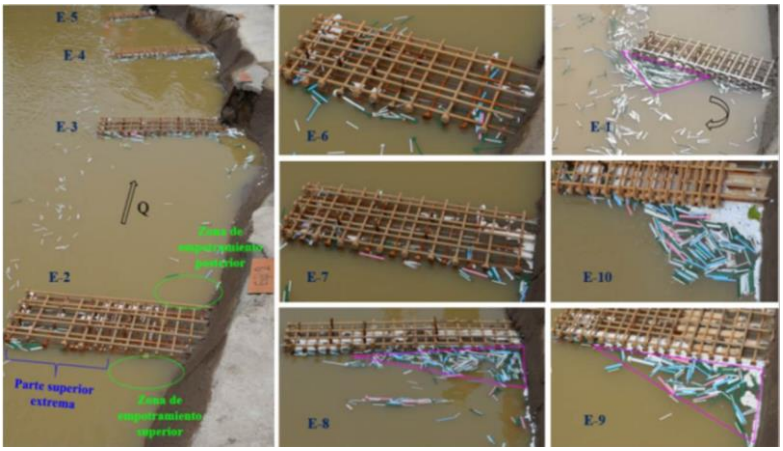

Figure 7. Accumulations of LWD upstream of ELJ groynes during Test 2. Notice accumulation patterns.

In this test 12 864 simulated LWD were incorporated into the flow. When the test was concluded 1 794 elements were trapped in the ELJ groyne field, which corresponds to 13.95 % of the elements that were incorporated into the flow. The largest deposition of simulated LWD occurred upstream of E-9 whereas a considerable amount was deposited upstream of E-1. Between E-1 and E-2 fewer units were deposited. This occurs because flow upstream of E-1 was diverted to the interior of the flume.

After the tests were concluded and water was slowly drained, it was noticed that most of the dowels were jammed at the maximum water level achieved during the tests. Blue arrows in Figure 9 show that a large number of simulated LWD were jammed on a horizontal line. Fewer units fell to the ground near the structure's anchors getting trapped by sand deposits starting to form a compact mix of sand and dowels.

Third test – Unsubmerged test

This test was conducted on February 24, 2017. Twelve ELJ groynes were placed on the right bank. All of the twelve ELJ groynes were placed on the right bank at a 90º. Total discharge was 514 L/s. Average velocity of flow in the curve was 0.38 m/s; estimated centrifugal force and Froude number were 0.36 KN and 0.294, respectively. In this test initial alignment of simulated LWD was similar to the First and Second Test. Simulated LWD ran faster near the left bank and most dowels approached the right bank as they moved in the downstream direction. Simulated LDW formed a narrow path impacting the tip of the groynes and forming clockwise vortices between groynes. Accumulation near the tips was rapidly and periodically removed by incoming flow and guided towards the right bank interior of the streambed. Most units were diverted downstream and the rest were temporarily trapped in between groynes.

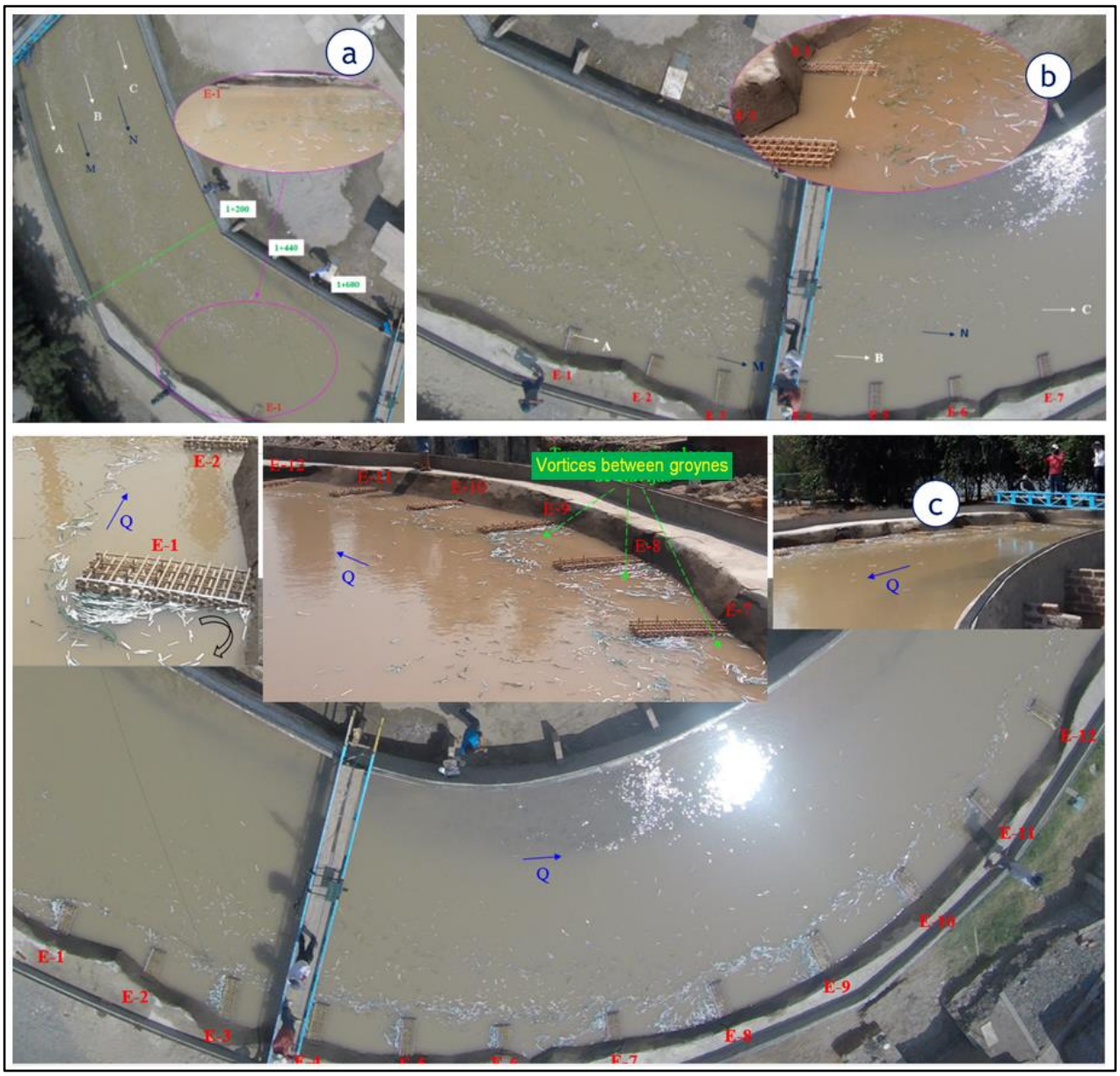

Figure 8. Flow and simulated LWD motion patterns in Test 3. Notice that simulated LWD approach the right bank and move near the tips of the ELJ groynes.

E-1 is the most critical ELJ groyne as it is exposed to impact by passing LWD. Drag forces (Fd) of simulated floating elements with and without disks were estimated as a function of their diameter Dt, angle with respect to the flow, θ, velocity on water surface, U, at point II, etc. Graphs in Figure 9 show estimated values of Fd as a function of angle of attack and Dt. Point II was located 10 cm upstream of the inner end of E-1. The location of this point can be seen in the figure 6c. E-1 is 1.25 m long.

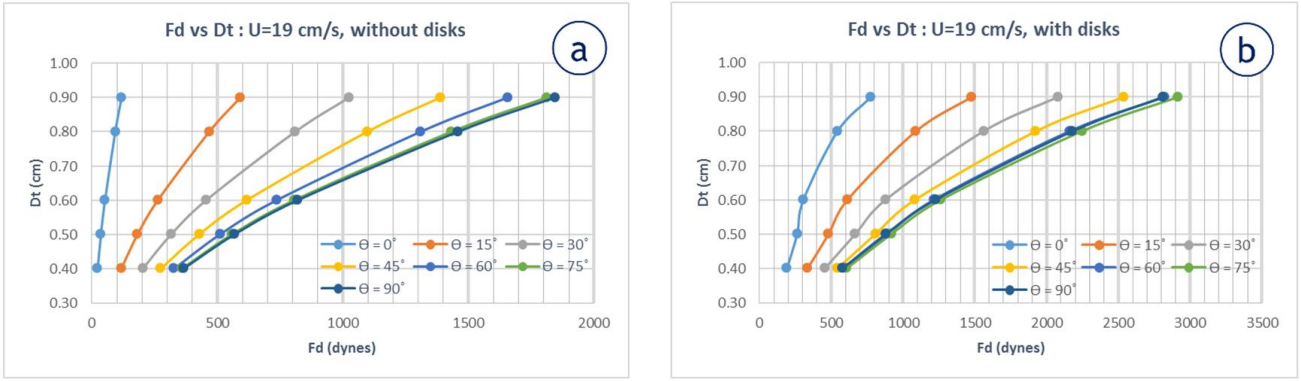

Figure 9. a) Fd vs Dt elements without disks. b) Fd vs Dt elements with disks. Third test.

When some dowels moved into a "dead zone", a few pieces remained in that position until the end of the tests. These dead zones were confined by the right bank and the upstream face of the ELJ groynes. Additional units were jammed in the interstices of the upstream face near or at the maximum water level attained.

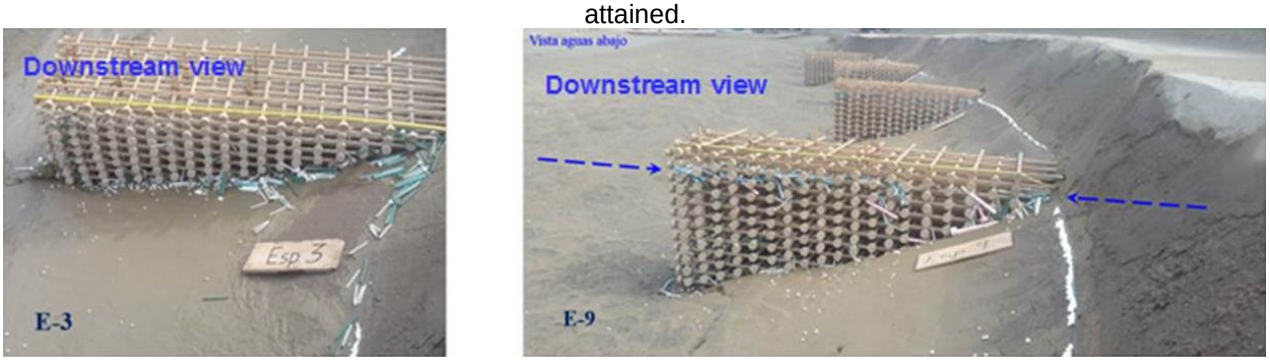

Figure 9. View of groynes E-3 and E-9 in the downstream direction. Notice dowels trapped in the upstream face of the groynes.

Table 5. Number of simulated LWD trapped upstream of ELJ groynes in Test 3.

ELJ Groyne		E-1	E-2	E-3	E-4	E-5	E-6	E-7	E-8	E-9	E-10	E-11	E-12	
Simulated LWD with disks	White, small	46	5	55	22	18	8	23	22	56	23	14	5	
	Green	2	1	18	19	11	17	6	11	30	21	20	6	
	Light blue	--	--	--	2	14	4	7	1	12	12	5	12	
	Pink	1	--	--	1	2	1	--	2	1	--	1	--	
	White, large	--	--	--	--	1	--	--	2	1	--	--	--	
Simulated LWD without disks	White, small	42	13	76	62	63	34	54	53	131	54	24	17	
	Green	25	9	98	46	35	7	24	23	67	53	25	18	
	Light blue	1	3	6	28	22	8	6	11	23	18	19	6	
	Pink	--	--	--	3	3	3	1	4	8	3	6	3	
	White, large	--	--	1	3	1	1	1	1	4	--	1	2	**Total trapped**
Partial quantity		117	31	254	186	170	83	122	130	333	184	115	69	1794
Partial % of total		0.91	0.24	1.97	1.45	1.32	0.65	0.95	1.01	2.59	1.43	0.89	0.54	13.95

4.2 Summary of main observations

In all tests simulated LWD closely followed the motion of the tracer's plumes that were injected into the flow prior to the incorporation of the elements simulating logs. As the flow entered the curve, separation between the tracer's plume and the left bank was evident in both cases. The tracer's plume moved towards the outer bank and a similar behavior was observed in the large mass of simulated LWD that was released into the flow. Individual elements remained approximately parallel to the main direction of the flow except when impacted by another element or when they were diverted towards the interior of the stream by a groyne. LWD was trapped in the groyne field when the structures were unsubmerged. Proportion of trapped material varied between tests as discharge and configuration slightly changed. Changes in configuration were related to the optimization of the training structures configuration. In the second test, 8 % of the simulated LWD passing through the river bend was trapped whereas in the third test 14 % of the simulated LWD was retained in the groyne field. A large number of elements where caught in the upstream face of the groynes near the maximum water level. A few dowels were deposited on embedment areas forming a hard mix with sediments.

5 PRELIMINARY RESULTS AND CONCLUSIONS

This article summarizes the results of a component of an experimental program in which the specific objective was to simulate the passage of LWD through a river meander and document the capacity of the groyne field to capture LWD. Trapped LWD over time may to replace parts of ELJ groynes. Three tests were conducted. In the first test, groynes were submerged and no elements were trapped. In the Second Test, trapping was uneven although the first ELJ groyne was able to capture a relatively large number of elements and also sustain significant impact. By the end of the Second Test, approximately 8% of the elements were trapped in the groyne field. In the Third Test, the groyne field was extended; covering the entire river bend and discharge was increased. By the end of this test, approximately 14 % of the simulated LWD was captured by the groyne field. Flow patterns were also observed and documented. Groyne fields placed on the outer bank of a bend trap logs in "dead zones", a corner formed by the upstream face of the ELJ groyne and the outer bank. When water was flowing, a triangle formed by the upstream face of the groyne, the outer bank of the watercourse and the simulated logs was observed. However, jamming of simulated LWD occurs mostly in the upstream face of a groyne. Most of the simulated logs get jammed at the maximum water level and structures'

permeability was barely affected. Experiments indicated that a groyne field placed in the outer bank of a river bend, over time, may trap woody material that may be used to repair ELJ groynes. The amount of captured material depends on the centrifugal force and the ELJ groyne field arrangement regardless of the number of elements in transit.

ACKNOWLEDGEMENTS
Funds for conducting most of the research program that included this component were partially assigned through Contract Nº 358-PNICP-PIAP-2014, subscribed between Universidad Nacional de Ingenieria (National University of Engineering) and the National Innovation Program for Competitiveness and Productivity, INNOVATE PERU. This program is sponsored by the Ministry of Production of Peru. The authors wish to express their gratitude to the students and research interns that participated in the experimental phase of this project such as: Alfredo Jacay, L. Antony Huaranca, Jhostyn Nina and Jhon Bautista. The participation of technical and administrative personnel at LNH is gratefully acknowledged. This paper summarizes part of the first author's thesis to obtain the Professional Title from the National University of Cajamarca (UNC). The second and third author guided his research efforts while the first author was a research intern at the National Hydraulics Laboratory. The fourth author was the first author's advisor at UNC.

REFERENCES

Abbe, T.B., Brooks, A.P., Montgomery, D.R. (2003) Wood in river rehabilitation and management. In: Gregory, S.V., Boyer, K.L., Gurnell, A.M. (Eds.), The ecology and management of wood inworld rivers. . American Fisheries Society, Symposium, vol. 37. Bethesda, Maryland, pp. 367-389.

Aragão, L. E. O. C., Malhi, Y., Metcalfe, D. B., Silva-Espejo, J. E., Jiménez, E., Navarrete, D., Almeida, S., Costa, A. C. L., Salinas, N., Phillips, O. L., Anderson, L. O., Alvarez, E., Baker, T. R., Goncalvez, P. H., Huamán-Ovalle, J., Mamani-Solórzano, M., Meir, P., Monteagudo, A., Patiño, S., Peñuela, M. C., Prieto, A., Quesada, C. A., Rozas-Dávila, A., Rudas, A., Silva Jr., J. A., and Vásquez, R. (2009) Above- and below-ground net primary productivity across ten Amazonian forests on contrasting soils, *Biogeosciences*, 6, 2759-2778, https://doi.org/10.5194/bg-6-2759-2009, 2009.

Araujo-Murakami, A., Parada, A. G., Terán, J. J., Baker, T. R., Feldpausch, T. R., Phillips, O. L., and Brienen, R. J. (2011). Necromasa de los bosques de Madre de Dios, Perú; una comparación entre bosques de tierra firme y de bajíos (In Spanish). *Revista Peruana De Biología*, 18(1), 113-118. https://doi.org/10.15381/rpb.v18i1.155

Braudrick, C. A., Grant, G. E., Ishikawa, Y. and Ikeda, H. (1997), Dynamics of Wood Transport in Streams: A Flume Experiment. Earth Surf. Process. Landforms, 22: 669-683. doi:10.1002/(SICI)1096-9837(199707)22:7<669::AID-ESP740>3.0.CO;2-L

Braudrick, C. A. and Grant, G. E. (2000) When do logs move in rivers? *Water Resour. Res.*, 36 (2), 571– 583, doi:10.1029/1999WR900290.

Chao, K.-J, Phillips, O. L., Baker T. R., Peacock J., Lopez-Gonzalez, G., Vasquez Martinez, R., Monteagudo, A. and Torres-Lezama, A. (2009) After trees die: quantities and determinants of necromass across Amazonia. *Biogeosciences Discuss.,* 6, 1979–2006, 2009.

Chuan, Walter (2019) Modelación Hidráulica del Transporte de Troncos Flotantes en el Meandro del Río Madre de Dios, Sector La Pastora – Puerto Maldonado. *Professional Title Thesis (in Spanish)*. School of Hydraulic Engineering. Universidad Nacional de Cajamarca. Cajamarca, Peru.

Consorcio Hidrovia Huallaga (2005) Estudio de la Navegabilidad en el Río Huallaga en el Tramo Comprendido Entre Yurimaguas y la Confluencia con el Marañón. Informe Final. Ministerio de Transportes y Comunicaciones. Lima, Peru.

Gurnell, A. M., Piégay, H., Swanson, F. J. and Gregory, S. V. (2002), Large wood and fluvial processes. Freshwater Biology, 47: 601-619. doi:10.1046/j.1365-2427.2002.00916.x

INDECI (2006). Mapa de Peligros de la Ciudad de Puerto Maldonado. Proyecto INDECI – PNUD PER / 02 / 051 Ciudades Sostenibles. Instituto Nacional de Defensa Civil. Lima, Perú.

Jacay, Alfredo César (2019) Diseño De Espigones Fabricados con Troncos de Árboles en el Río Madre de Dios. *Professional Title Thesis (in Spanish)*. School of Civil Engineering. Universidad Nacional de Piura. Piura, Peru.

NCHRP (2010). Effects of Debris on Bridge Pier Scour. Report 653. National Cooperative Highway Research Program Transportation Research Board, 9-50.

Pfister, M; Capobianco, D; Tullis, B. and Schleiss, A.J. (2013) Debris-Blocking Sensitivity of Piano Key Weirs under Reservoir-Type Approach Flow. J. Hydraul. Eng, (139) 11.

Ruiz-Villanueva, V., Castellet, E. B., Díez-Herrero, A., Bodoque, J. M., & Sánchez-Juny, M. (2014) Two-dimensional modelling of large wood transport during flash floods. *Earth Surf. Process. Landforms* 39, 438–449 (2014)

Shields, F.D., Morin, N., Cooper, C.M. (2004) Large Woody Debris Structures for Sand-Bed Channels. J. Hydraul. Eng 130(3)

Wohl, E. (2013). Floodplains and wood. Earth-Science Reviews, 194–212.